Title: Label-free optical biosensor for real-time monitoringthe cytotoxicity of xenobiotics: A proof of principle study on glyphosate

Authors: Eniko Farkas, Andras Szekacs, Boglarka Kovacs, Marianna Olah, Robert Horvath, Inna Szekacs

PII: S0304-3894(18)30133-X
DOI: https://doi.org/10.1016/j.jhazmat.2018.02.045
Reference: HAZMAT 19209

To appear in: *Journal of Hazardous Materials*

Received date: 24-7-2017
Revised date: 8-2-2018
Accepted date: 23-2-2018

Please cite this article as: Farkas E, Szekacs A, Kovacs B, Olah M, Horvath R, Szekacs I, Label-free optical biosensor for real-time monitoringthe cytotoxicity of xenobiotics: A proof of principle study on glyphosate, *Journal of Hazardous Materials* (2010), https://doi.org/10.1016/j.jhazmat.2018.02.045

Label-free optical biosensor for real-time monitoringthe cytotoxicity of xenobiotics: a proof of principle study on glyphosate

Eniko Farkas[a,b], Andras Szekacs[c], Boglarka Kovacs[a,b], Marianna Olah[c,d], Robert Horvath[a*], Inna Szekacs[a*]

[a]*Nanobiosensorics Momentum Group, Institute of Technical Physics and Materials Science, Centre for Energy Research, Hungarian Academy of Sciences, Konkoly-Thege M. u. 29-33, H-1120 Budapest, Hungary*
[b]*Subdoctoral School of Molecular and Nanotechnologies, Chemical Engineering and Material Science Doctoral School, University of Pannonia, Egyetem u.10, H-8200 Veszprém, Hungary*
[c]*Agro-Environmental Research Institute, National Agricultural Research and Innovation Centre, Herman Ottó u. 15, H-1022 Budapest, Hungary*
[b]*Doctoral School of Environmental Sciences, Szent István University, Páter K. u.1, H-2100 Gödöllő, Hungary*

* E-mails: horvathr@mfa.kfki.hu, szekacs.inna@energia.mta.hu

Graphical abstract

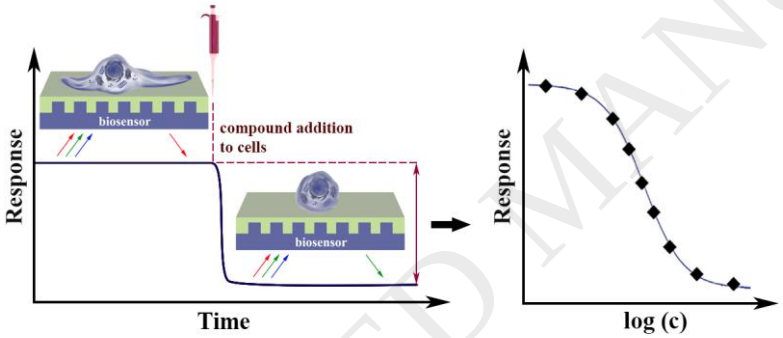

Highlights

- A real-time label-free biosensor technique for measuring cytotoxicity was developed.
- Effects of herbicide Roundup Classic, its formulant POEA and active ingredient glyphosate were determined on adhered cells.
- A surface sensitive optical biosensor detects and provides unique information about cytotoxicity.
- The approach was validated by conventional bioassays.
- Biosensor and cell morphology results are indicative of a certain synergy between glyphosate and POEA in Roundup Classic.

Abstract

Rapid and inexpensive biosensor technologies allowing real-time analysis of biomolecular and cellular events have become the basis of next-generation cell-based screening techniques. Our work opens up novel opportunities in the application of the high-throughput label-free Epic BenchTop optical biosensor in cell toxicity studies. The Epic technology records integrated cellular responses about changes in cell morphology and dynamic mass

redistribution of cellular contents at the 100-150 nm layer above the sensor surface. The aim of the present study was to apply this novel technology to identify the effect of the herbicide Roundup Classic, its co-formulant polyethoxylated tallow amine (POEA), and its active ingredient glyphosate, on MC3T3-E1 cells adhered on the biosensor surface. The half maximal inhibitory concentration of Roundup Classic, POEA and glyphosate upon 1 h of exposure was found to be 0.024%, 0.021% and 0.163% in serum-containing medium and 0.028%, 0.019% and 0.538% in serum-free conditions, respectively (at concentrations equivalent to the diluted Roundup solution). These results showed a good correlation with parallel end-point assays, demonstrating the outstanding utility of the Epic technique in cytotoxicity screening, allowing not only high-throughput, real-time detection, but also reduced assay run time and cytotoxicity assessment at end-points far before cell death would occur.

Keywords: label-free biosensor, resonant waveguide grating, glyphosate, polyethoxylated tallow amine, cytotoxicity

1. Introduction

Xenobiotics (such as drugs, pesticides and environmental pollutants) are chemical substances foreign to the biological systems [1,2]. Adverse toxicity of biologically active substances, e.g. pesticide active ingredients (among others, amitraz, dichlorvos, and glyphosate) have been found [3–5], and as novel toxic side-effects are identified, new xenobiotics also become subject to increasingly strict toxicity assessment. Synthetic chemicals of poor toxicity profile, approved on the basis of their earlier, less restrictive registration, to date remain in use, as no replacement substances have yet been found. A herbicide active ingredient glyphosate and its formulated plant protection product Roundup, having lately been in the focus of vocational and societal debates in risk assessment, were chosen for the present study to assess its biological effects on adhered cells by a label-free biosensor technique.

Since its first registration in 1974, glyphosate has widely been applied in agriculture. Its use has drastically increased during the last three decades, boosted also by the use of glyphosate-resistant genetically modified (GM) crops [6,7], and by now it is the leading pesticide active ingredient worldwide [5]. However, the intensive use of pesticide preparations containing this compound has led to both environmental and health effects. Due to its increasing chemical load on the environment [7], the presence of glyphosate has been detected and reported by several studies in soil [8] and surface water [9]. Glyphosate decays differently in soft and hard water: its half-life is a few weeks in normal water, but may increase to years in hard water due to complexation with Ca^{2+} ions [10]. Both glyphosate and its decomposition product aminomethylphosphonic acid (AMPA) present hazard to the aqueous ecosystem [9]. In ecological response to the exhaustive use of glyphosate-based herbicides, new glyphosate-resistant weed species have appeared and biodiversity losses occurred [11]. In addition, increased glyphosate dosages due to resistant weeds or number of applications on GM crops led to elevated levels of glyphosate residues in the crops treated; and such herbicide contaminated plants are being used as animal feed or in food production. In turn, occurrence of herbicide residues were reported in meat produced [12] and in other

foods as well [13]. Human exposure, indicated also by glyphosate residues detected in human urine [14], may lead to health harms potentially associated with exposure to glyphosate or formulated glyphosate-based herbicides. Numerous diseases have been hypothesized to be possibly induced by glyphosate or its herbicide formulations, e.g. renal failure [15], autism [16], celiac incidence [17], asthma [18], allergy [19], cancer [20], diabetes [15], endocrine diseases [21], intestinal infection [22] or birth abnormalities [23,24]. Several of these diseases or disorders are directly related to cellular toxicity, therefore, cytotoxicity to hepatic, hematopoietic, bone marrow, neuronal, fetal and embryonal, placental and other cell lines has become a crucial issue in risk assessment of glyphosate and glyphosate-based herbicides [25–30].

Cytotoxic effects of glyphosate and glyphosate-based herbicides have been mainly examined with traditional toxicity assays (MTT and cell proliferation tests [31,32], enzyme activity assays [21,32]). But, classical methods in cytotoxicity assessment are time-consuming, material- and labor-intensive, predominantly apply labeling, and their ability to measure in serum-free conditions is limited. Nowadays, the rapid and inexpensive biosensor technology performed in real-time has become the basis of new-generation cell-based techniques, applicable with both prokaryotic (bacteria) and eukaryotic (yeast, invertebrate and vertebrate, mammalian) cells, and capable to indicate organic and inorganic environmental pollutants including genotoxic, ecotoxic or endocrine disrupting xenobiotic compounds [33–38]. Biosensors detect cellular responses to a given compound by monitoring interactions between cell membrane receptors and toxins, cell signaling, cell morphology and cell–surface interactions, and thus, collect information about the functional state of surface-attached cells. These changes can be detected by electrochemical (impedimetric [39–41], voltammetric [42,43], amperometric [44–46], and potentiometric [47,48]) biosensors. These integrated devices provide analytical information by recognition of biological events involving an electrochemical transducer [49].

An acoustic sensor setup, quartz crystal microbalance (QCM), has been applied for drug discovery [50,51], clinical diagnostics [52,53], toxicity assessment [54], monitoring biochemical and cellular processes [55]. The operating principle of QCM is based on recording changes in the resonant frequencies of a piezoelectric quartz crystal, proportional to the mass change at the sensor surface. Simply, mass gains on the crystal due to surface interactions cause a shift towards lower oscillation frequencies. Advantages of the QCM are real-time kinetic information, without the need for labeling, moreover, the method is inexpensive and easily integrable into portable devices [54].

Another novel non-invasive technique for quantifying cytotoxicity is digital phase contrast time-lapse microscopy, often called holographic microscopy or HoloMonitor. Today, the method is available as a small footprint device, easily applicable in a humidified cell culture incubator. This novel tool is capable to follow cell morphological changes, connected to important cellular events, including adhesion, proliferation, migration, differentiation, and death [56,57]. The technique is based on a Mach-Zender interferometer setup using a reference and an object laser beam. Due to interactions with sample components, a phase delay occurs in the object laser beam passing through the sample reference to the sample beam. By interfering the two beams a hologram is created, from which the positions and shapes of individual cells can be numerically calculated. Therefore, the method allows label-

free recording of three-dimensional (spatial) images of single cells and cell populations. A limitation is, however, that the process is relatively low throughput and cost per data point is high, which may represent an important issue for given screening settings [58,59].

Assessment of toxicity of xenobiotics can also be detected optically by employing surface plasmon resonance [60–64], optical waveguide lightmode spectroscopy [65–67], photonic crystal biosensor [68–71], and resonant waveguide grating (RWG) [72–75]. These techniques use an evanescent electromagnetic field to detect refractive index changes at the sensor surface. The cell-based detection with these techniques is usually limited to a sample probing depth of ~150 nm, so only the very bottom portion of the cells, in the nearest contact with the sensor surface, could be sensed. Non-commercialized reverse symmetry waveguide configurations were demonstrated, however, with larger and tunable probing depths [76,77].

A commercially available RWG optical biosensor, the Epic BenchTop (BT) has already been proven to be a powerful tool for high-throughput label-free detection of cell adhesion, spreading and signaling events [72,78–81] in real-time and quantitative evaluation. RWGs open up opportunities in novel cell toxicity assays, too. This non-invasive technique is available for high-throughput screening by using 96- or 384-well microplates with a single optical biosensor in each well [82]. The Epic BT was mainly used for cell and biochemical measurements [82]. The Epic system measures the integrated cellular events taking place within the sensing region; changes in cell morphology and in protein redistributions within the probing depth are often termed as dynamic mass redistribution (DMR) [72]. This versatile biosensor was chosen to be applied in our study, because it provides detailed information on the binding affinity [80], kinetics of interactions [78,81] and the biological status of cells (e.g., cell viability, cell density, and degree of adhesion) [82].

A current problem in ecotoxicology is that environmental and toxicological characteristics of formulated pesticides may substantially differ from those of their active ingredients or other components alone. It has been suggested that certain toxic effects of glyphosate-containing herbicides were related to the surfactant components of the formulated products [28,32]. Studies indicate that the surfactant polyoxyethyleneamine or polyethoxylated tallow amine (POEA), used in some commercial glyphosate-based formulations, is far more toxic than glyphosate itself [5,32,83,84]. The mechanism of the toxicity of glyphosate in mammals is unknown, and hypotheses have been disputed.

In the present work, the herbicide product Roundup Classic, its formulant (POEA) and its active ingredient (glyphosate) were studied on a mammalian osteoblastic cell line (MC3T3-E1) model using the optical biosensor Epic BT. Cell viability was monitored by HoloMonitor M4 time-lapse cytometer and Muse Cell Analyzer. Here, we demonstrate for the first time the efficacy of the Epic BT biosensor method as a label-free screening technique for rapid quantification of cytotoxicity. This method provides ability to measure whole-cell responses directly, in real-time, using serum-containing and serum-free environments, and could be potentially useful for first-step screening of cytotoxic effects of xenobiotics. Moreover, we subsequently validate the data obtained from the Epic assays with microscopic and flow cytometric techniques.

2. Materials and methods

2.1. Chemicals

All chemicals and reagents were obtained from Sigma-Aldrich, unless stated otherwise. Glyphosate (in form of its isopropylammonium salt) analytical standard used was Pestanal grade, from Riedel-de Haën (Seelze, Germany), Roundup Classic was purchased from public commercial source, and POEA was received from Lamberti SpA (Albizzate, Italy). A stock solution of Roundup Classic and equivalent solutions of glyphosate and POEA were prepared freshly in 20 mM 4-(2-hydroxyethyl)-1-piperazine ethanesulfonic acid (HEPES) Hank's balanced salt solution (HBSS) buffer or in serum-containing cell culture medium, the pH was adjusted to pH 7.4 if needed, and solutions were filtered through a filter (0.22 μm).

2.2. Cell culture

The osteoblastic cell line MC3T3-E1 (93021013 Sigma-Aldrich) was maintained in α-modified minimal essential medium (α-MEM), supplemented with 10% fetal bovine serum (FBS, Biowest SAS, France), 2 mM L-glutamine, 100 U/ml penicillin and 100 μg/ml streptomycin solution, and 0.25 μg/ml amphotericin B. Cells were cultured in a humidified atmosphere containing 5% CO_2 at 37°C. On reaching 80% confluence, cells were detached every 3-4 days using 0.05% (w/v) trypsin, 0.02% (w/v) EDTA solution and not used beyond passage 20.

For the Epic assay MC3T3-E1 cells were removed from tissue culture dishes using trypsin-EDTA, counted and diluted in complete growth medium (α-MEM+10% FBS), and were seeded at 10,000 cells per well in 25 μl into 384-well Epic Cell Assay Microplates (#5040, Corning Incorporated, Corning, NY, USA). Cells were let attach to the sensor surface for overnight in a humidified incubator for formation of a confluent monolayer. Following the overnight incubation, assays in serum-containing medium were carried out in microplates with attached cells in the complete growth medium being placed in the Epic reader for measurements. For assays under serum-free conditions, the culturing medium in the microplate was replaced with 25 μl per well 20 mM HEPES HBSS (pH 7.4) prior to measurement.

2.3. Epic biosensor technique

All measurements were performed in 384-well Epic cell assay microplates (Corning Incorporated, Corning, NY, USA). The bottom of each well of the microplate contains a 2x2 mm RWG sensor. The grating areas couple the incident light into a Nb_2O_5 waveguiding layer and thus, an evanescent optical field decaying exponentially with the distance from the sensor surface (with a penetration depth of 150 nm) is created. The characteristic wavelength, at which the resonant evanescent field is created (i.e., the resonant wavelength, λ), is affected by any changes in the refractive index inside the penetration depth of the TM_0 mode. Cellular responses induce refractive index changes and shift the resonance to a new wavelength ($\lambda' \neq \lambda$) resulting in a resonant wavelength shift ($\Delta\lambda = \lambda' - \lambda$). $\Delta\lambda$ is proportional to the alteration in the effective refractive index of the substrate-cell-medium system. These processes can be followed in real-time with very high resolution. The employed microplate format allows 384 parallel measurements by reading the resonant wavelength between 825 and 840 nm in every

3 s in each well. Moreover, the distribution of the resonant wavelength is imaged in each well by using a high speed complementary metal oxide semiconductor camera [72].

2.4. Epic assay

Prior to reagent addition, a baseline was recorded in the wells of the Corning Epic sensor microplate for approximately 1 h in 25 µl assay medium (α-MEM+10% FBS or 20 mM HEPES HBSS, pH 7.4). Upon stable baselines having been established for all wells, 25 µl of sample solutions were added from a source plate to the attached cells in the Epic plate or to wells containing only assay medium for compound control using an electronic 16-channel pipette Finnpipette™ Novus (Thermo Fisher Scientific, Waltham, MA, USA) in stepping mode. Biosensor responses were recorded for 1 h. To compensate for the effect of the compound addition on the refractive index of the medium, DMR signals obtained in wells containing cells treated with a reagent were corrected with corresponding DMR signals obtained in wells containing assay medium and the reagent at the corresponding concentration (compound control). This correction also compensates for physical influences, e.g. temperature and dilution effects. A similar compensation was applied to wells containing untreated MC3T3-E1 cells (cell control) corrected by DMR signals of the assay medium. All measurements were replicated at least three times at room temperature.

2.5. Epic data analysis

Once the assay was completed, DMR signals for each treatment were obtained by averaging triplicates and correcting to the respective reagent control as described above. Assay signals obtained during the incubation time were calculated as the difference between the DMR signal after 1 h of compound addition and the corresponding baseline. Dose response curves for different compounds were obtained by plotting assay signals obtained for treatments at various concentrations of the given compound. In the case of high reagent concentrations, when lysis of the cells can occur and cause mass increase on the sensor surface, the lowest DMR signal was used for assay signal calculation.

2.6. Determination of cell viability/cytoskeletal organization by fluorescence microscopy

After the measurements with Epic biosensor, cells in the sensor microplates were fixed with 4% paraformaldehyde and stained with Actin Cytoskeleton and Focal Adhesion Staining Kit (Merck Millipore, Budapest, Hungary). The kit applied consists of TRITC-conjugated phalloidin, anti-vinculin and DAPI, which could visualize actin filaments in the cytoskeleton, focal contacts and the nucleus of the cells respectively. Cells were observed in fluorescent mode with a Zeiss Axio Observer.Z1 microscope using a 20× objective.

2.7. Determination of cell viability by HoloMonitor M4

Cell morphology of MC3T3-E1 cells was studied using label-free time-lapse cytometer HoloMonitor M4 (Phase Holographic Imaging AB, Lund, Sweden) [59]. Cells were seeded at a density of 100,000 cells per channel (2.5 cm^2) of Ibidi µ-Slide I ibiTreat (#80106, tissue

culture treated, Ibidi) in complete growth medium and were cultured overnight in a humidified incubator. The solutions of Roundup Classic, POEA and glyphosate were prepared freshly in complete growth medium, the pH was adjusted to 7.4 if needed, and the solutions were filtered through a filter (0.22 μm). Following overnight incubation of cells, culturing medium was changed to assay medium containing the target substances at the required concentrations. Three-dimensional structures of cells were visualized in a HoloMonitor M4 digital holographic microscope by sample illumination with 0.1 mW/cm^2 HeNe laser (635 nm). The interference pattern was recorded as a hologram on a digital sensor. Images were captured every 5 min inside a humidified incubator. Video was prepared using software HoloStudio M4.

2.8. Apoptosis detection using Muse Caspase 3/7 kit

MC3T3-E1 cells were grown in 24-well plate for overnight in a humidified incubator followed with the cell treatment with different concentration of the reagents. Floating and adherent treated cells were collected after 24 h incubation. Subsequently, the cells were labeled with Muse Caspase 3/7 kit according to the manufacturer's instructions (Merck Millipore). This assay provides relative percentage of cells that are live, in the early and late stages of apoptosis, and dead. The samples were counted by the Muse Cell Analyzer (Merck Millipore, Budapest, Hungary).

3. Results and discussion

3.1. Epic BT measurements

Toxic effects of environmental chemicals can lead to passive cell death or result in the active mechanism of apoptosis. These integrated cellular events can be detected with biosensor techniques through differences in the kinetics of processes induced by the given xenobiotic on the sensor surface [85]. Thus, the effects of varying concentrations of Roundup Classic, glyphosate and POEA on MC3T3-E1 cells were investigated using the Epic BT. Because the assay solution composition (i.e., completed culturing medium contains additional factors, lipids, minerals, and proteins) could interfere with the reagents, experiments were performed in both serum-containing and serum-free conditions. The cells were let to attach to the sensor surface for overnight in a humidified incubator followed by baseline recording in an Epic BT instrument, and the reagents were added at different concentrations in an appropriate assay medium.

The cell death profile is typically revealed as a significant negative shift in the DMR signal through cell size reduction, weakening adhesion strength, and detachment from the sensor surface [69]. Exposing cells to 0.1% Roundup Classic and 0.016% POEA (equivalent to 0.1% Roundup Classic) induced a large negative DMR response in MC3T3-E1 cells under serum-containing (**Fig. 1A**) and serum-free (**Fig. 1B**) conditions, which reached its negative maximum in about 10 minutes after reagent addition. Note, 150 pm wavelength shift corresponds to a refractive index change of 0.0013 inside the sensing zone, as established earlier by calibrating the Epic BT using a table top refractometer [86]. The relatively slow kinetics in the upward drift region in the DMR response after reaching negative maximum,

seen at the highest concentrations of Roundup Classic applied is possibly due to cell lysis. As shown in **Fig. 1A**, kinetics of the biosensor response to Roundup Classic and POEA at equivalent concentrations had a similar-shaped dependency, supposedly due to cell death, lysis and/or detachment. The magnitude of the signal was found to be dose-dependent, with the lowest signal observed with the highest dose of Roundup Classic or POEA. Exposing cells to 0.042% glyphosate (equivalent to 0.1% Roundup Classic) in serum-containing medium (**Fig. 1A**) caused late phase response on MC3T3-E1 cells, possibly due to cell cytoskeletal reactions. The higher the glyphosate concentration is, the earlier the decrease in the Epic signal occurs. However, no significant effect was observed for glyphosate at 0.042% concentration in serum-free condition (**Fig. 1B**). These results suggest that the toxic effect of Roundup Classic is likely to be attributed to POEA and possibly influenced by glyphosate. **Figs. 1C** and **1D** show dose-dependent responses of MC3T3-E1 cells to Roundup Classic, glyphosate and POEA from the measurements in serum-containing and serum-free assay media, respectively.

Table 1 summarizes the EC_{50} values obtained for Roundup Classic, POEA and glyphosate. No significant differences were observed in the IC_{50} values of Roundup Classic and POEA in both assay media. In contrast, the IC_{50} value of 0.068% for glyphosate in a serum-containing medium (α-MEM+10% FBS) appeared to be almost twice as low as under serum-free conditions (0.223%). As the serum is known to contain a high amount of proteins that can attenuate the effects of toxicants through binding [87], one would expect lower effects in serum-containing medium, than under serum-free conditions. Surprisingly, however, the results obtained with glyphosate showed higher impact in serum-containing medium. To exclude the possibility that this difference is due to pH changes in the serum-containing medium [65] as it did not contain any HEPES for buffering at room conditions, the pH of the medium was checked during the 1-h measurement, and no changes were observed.

To demonstrate the advantages of the real-time Epic technique and to demonstrate its sensitivity, MC3T3-E1 cells exposed to the same compounds were also examined with fluorescence and holographic microscopy, and cytometry techniques.

3.2. Fluorescence microscopy

At the end of the previously showed Epic measurements, cells were fixed directly in the sensor microplates and stained to visualize morphological changes. Comparing to the control group (**Fig. 2A**) the shape of glyphosate-treated cells became elongated (**Fig. 2B**), and the treatment resulted in a reduction in the distribution of F-actin. This suggests, that glyphosate influences cell adhesion and morphology of the cytoskeleton. As phosphorus ligands are known to have strong affinity for bivalent metal ions (i.e., Ca^{2+} and Mg^{2+}) [88], glyphosate at high concentrations promotes cation (Ca^{2+}) chelating efficiency, which takes effect on the cell adhesion, cytoskeletal localization and morphology [89,90]. In fact, AMPA and its derivatives, among them glyphosate, had been patented as chemical chelators in 1964, as they bind and remove minerals such as calcium, magnesium, manganese, copper, and zinc [91].

Nonetheless, glyphosate is a relatively weak (3 times less effective) Ca^{2+} and Mg^{2+} cation chelator compared to EDTA [92], indicating that chelating affinity can only partially contribute to the effect of cell detachment and morphology alterations caused at high concentrations of glyphosate. In contrast, POEA (**Fig. 2C**) caused cellular plasma membrane permeabilization, cytoskeletal collapse and cell death, and it showed more cytotoxic effect than glyphosate or Roundup Classic. Moreover, necrosis also occurs as an effect of POEA on the cells [93]. **Fig. 2D** illustrates the effect of Roundup Classic causing morphological changes in the cells similar to those occurring upon exposure to POEA. This similarity indicates that the effect of POEA mainly prevails in Roundup Classic. The images obtained by fluorescence microscopy confirmed the results of the Epic measurements.

3.3. Cell morphology study by HoloMonitor time-lapse cytometry

Our preliminary results have demonstrated the utility of the HoloMonitor technique to be applied for determination of cytotoxicity [56], acknowledged and implied by the manufacturer [94]. The representative images obtained in this study at 5 min, 1 h and 24 h of cell incubation are shown in **Fig. 3**. Control cells showed a flat, elongated shape (**Fig. 3A**), proliferated exponentially (**Fig. 4A**), maintained migration dynamics (**Fig. 4B**), and the average cell population optical thickness indicated monolayer formation (**Fig. 4C**). While proliferation of cells treated with 0.02% Roundup Classic was inhibited, cells become rounded (**Figs. 3B, 4A**). The analysis of morphological data demonstrates that during treatment with 0.02% Roundup Classic the average optical thickness of the cell population substantially increased after 1 h indicating cells proceeding to apoptosis (**Fig. 4C**). After 24 h of treatment, this value increased by 2-fold compared to the values at the beginning of the treatment. Treatment with POEA (0.003%, equivalent of 0.02% Roundup solution) led to a massive drop in cell area after 5 min (**Fig. 3C**) and showing cell necrosis after 1h of incubation. Mesnage et al. demonstrated that POEA, as one of the components in Roundup formulations, induced human toxicity, triggered necrosis by disrupting cell membranes around its critical micellar concentration, rather than glyphosate, that led to apoptosis [95]. Treating cells with 0.008% glyphosate (equivalent of 0.02% Roundup solution) didn't show significant alternations from control cells (**Fig. 3D**, **Fig. 4**). While 0.5% glyphosate led to impaired cell mobility, growth of cell height (**Fig. 3E, 4E**) and inhibition of cell division (**Fig. 4A**), cells still kept some migration dynamics (**Fig. 4B**), and these changes are likely to be due to exerting a cytostatic effect.

3.4. Cell viability measurement with Caspase 3/7

Similar behaviors of the xenobiotics studied were observed using the Muse Caspase 3/7 Cell Viability Test. The measurement setup and the apoptosis profiles are shown for each reagent in **Fig. 5**. The ratio of apoptotic cells is higher in cells exposed to POEA and Roundup Classic than in cells treated with glyphosate at equivalent concentrations (**Fig. 5A, B**). These results correlated with the previous results, showing that glyphosate-treated cells keep their viability. The measurement also demonstrated that POEA induces cell death at much lower concentration than in Roundup Classic. IC_{50} values (upon 24 h of exposure) in equivalents of

diluted Roundup Classic solutions were calculated and resulted in 0.007% for Roundup Classic and 0.006% for POEA (0.001% or 0.011 mM actual POEA concentration) (**Fig. 5C**). It has to be noted that caspase 3/7 activities could not be determined at concentrations above 0.01% of Roundup Classic and POEA, as total cell death has been reached by this concentration. In contrast, glyphosate caused only 17% decrease in caspase 3/7 activity at a concentration in equivalent to 1.2% of diluted Roundup Classic (0.5% or 21.9 mM actual glyphosate concentration).

4. Conclusions

In summary, the Epic BT biosensor was first employed to measure the biological effects of the worldwide used herbicide Roundup Classic and its components, active ingredient glyphosate and additive surfactant POEA, on adhered cells in serum-containing and serum-free conditions. The obtained quantitative data suggest that the Epic biosensor detects and provides unique information about cytotoxicity. The benefits of the presented approach are online direct detection of biochemical and cellular events, without the need for any labeling. This setting avoids experimental uncertainty due to possible effects of the label during an experiment. We proved that the introduced detection method greatly shortens assay time and simplifies cytotoxicity assessment at end-points far before cell death would occur. These advantages make our biosensor method suitable as alternative test for toxicology screening and for supplementing conventional methods.

From the biosensor signals half maximal inhibitory concentration of the biological function was determined for each agent using sigmoidal curve fits. The results from Epic BT biosensor showed good correlation with the conventional methods. Glyphosate has to be applied at higher concentration than Roundup Classic or POEA to exert cytotoxicity. The results obtained indicate that POEA strongly influences morphology and integrity of the cells, causes apoptotic and necrotic effects, while glyphosate influences effects of cell adhesion and cytoskeleton morphology. Holographic microscopy revealed that glyphosate at levels equivalent to concentrations of Roundup Classic used in agriculture, or somewhat below, influences cell division, motility, elongated morphology, and causes cell death (although slower than that caused by POEA and Roundup Classic). Moreover, our biosensor data and observations in cell morphology are indicative of a certain synergy between glyphosate and POEA in Roundup Classic product. It is important to emphasize that Roundup Classic is used in agricultural work at dilutions ranging from 1% to 2%, concentrations two orders of magnitude higher than those described in our results.

Several aspects revealed in this study need to be further investigated. There occurs no simple correlation between the effects of Roundup Classic and its components: although a similarity is observed between the effects of Roundup Classic and POEA, glyphosate appears to cause different cellular effects. Moreover, the mechanism of the effect of glyphosate on MC3T3-E1 cell adhesion also deserves further, more in-depth assessment.

Acknowledgements

The present work was supported by the Lendület (Momentum) Program of the Hungarian Academy of Sciences, by the ERC_HU Program of NKFIH and by project K109865 by the Hungarian Scientific Research Fund (OTKA).

References

[1] A. Iovdijová, V. Bencko, Potential risk of exposure to selected xenobiotic residues and their fate in the food chain-part I: Classification of xenobiotics, Ann. Agric. Environ. Med. 17 (2010) 183–192. http://www.ncbi.nlm.nih.gov/pubmed/21186759 (accessed June 30, 2017).

[2] Moltmann J.F. and Rawson D.M., Applied ecotoxicology, CRC Press, 1995.

[3] C. Ramel, J. Drake, T. Sugimura, An evaluation of the genetic toxicity of dichlorvos, Mutat. Res. Genet. Toxicol. 76 (1980) 297–309. doi:10.1016/0165-1110(80)90021-4.

[4] A.T. Proudfoot, Poisoning with amitraz, Toxicol. Rev. 22 (2003) 71–74. doi:10.2165/00139709-200322020-00001.

[5] A. Székács, B. Darvas, Forty Years with Glyphosate, Herbic. Synth. Control Weeds. (2012) 247–284. doi:10.5772/32491.

[6] S.O. Duke, S.B. Powles, Glyphosate-resistant crops and weeds: Now and in the future, AgBioForum. 12 (2009) 346–357.

[7] L.L. Wolfenbarger, P.R. Phifer, The Ecological Risks and Benefits of Genetically Engineered Plants, Science (80-.). 290 (2000) 2088–2093. doi:10.1126/science.290.5499.2088.

[8] M.A. Weaver, L.J. Krutz, R.M. Zablotowicz, K.N. Reddy, Effects of glyphosate on soil microbial communities and its mineralization in a Mississippi soil, Pest Manag. Sci. 393 (2007) 388–393. doi:10.1002/ps.

[9] U. Reno, L. Regaldo, E. Vidal, M. Mariani, C. Zalazar, A.M. Gagneten, Water polluted with glyphosate formulations: Effectiveness of a decontamination process using Chlorella vulgaris growing as bioindicator, J. Appl. Phycol. 28 (2016) 2279–2286. doi:10.1007/s10811-015-0755-6.

[10] C. Jayasumana, S. Gunatilake, P. Senanayake, Glyphosate, hard water and nephrotoxic metals: Are they the culprits behind the epidemic of chronic kidney disease of unknown etiology in Sri Lanka?, Int. J. Environ. Res. Public Health. 11 (2014) 2125–2147. doi:10.3390/ijerph110202125.

[11] R.A. Relyea, The impact of insecticides and herbicides on the biodiversity and productivity of aquatic communities, Ecol. Appl. 15 (2005) 618–627. doi:10.1890/03-5342.

[12] A.Z. Dinon, D. Treml, C.S. de Mello, A.C.M. Arisi, Monitoring of GMO in Brazilian processed meat and soy-based products from 2007 to 2008, J. Food Compos. Anal. 23 (2010) 226–229. doi:10.1016/j.jfca.2009.12.002.

[13] A.A. Selvi, M.A. Sreenivasa, H.K. Manonmani, Enzyme-linked immunoassay for the detection of glyphosate in food samples using avian antibodies, Food Agric. Immunol. 22 (2011) 217–228. doi:10.1080/09540105.2011.553799.

[14] L. Niemann, C. Sieke, R. Pfeil, R. Solecki, A critical review of glyphosate findings in human urine samples and comparison with the exposure of operators and consumers, J. Consum. Prot. Food Saf. (2014). doi:10.1007/s00003-014-0927-3.

[15] N.L. Swanson, A. Leu, J. Abrahamson, B. Wallet, Genetically engineered crops,

glyphosate and the deterioration of health in the United States of America, J. Org. Syst. Abrahamson Wallet J. Org. Syst. 9 (2014) 6–37.

[16] J.E. Beecham, S. Seneff, Is there a link between autism and glyphosate-formulated herbicides?, J. Autism. 3 (2016) 1. doi:10.7243/2054-992X-3-1.

[17] A. Samsel, S. Seneff, Glyphosate, pathways to modern diseases II: Celiac sprue and gluten intolerance, Interdiscip. Toxicol. 6 (2013). doi:10.2478/intox-2013-0026.

[18] D.P. Sandler, J.A. Hoppin, Exacerbation of symptoms in agricultural pesticide applicators with asthma, Int Arch Occup Env. Heal. (2013). doi:10.1007/s00420-013-0881-x.

[19] E. Sten, P.S. Skov, S.B. Andersen, A.M. Torp, A. Olesen, U. Bindslev-Jensen, L.K. Poulsen, C. Bindslev-Jensen, A comparative study of the allergenic potency of wild-type and glyphosate-tolerant gene-modified soybean cultivars, Apmis. 112 (2004) 21–28. doi:10.1111/j.1600-0463.2004.apm1120104.x.

[20] P.J. Mink, J.S. Mandel, B.K. Sceurman, J.I. Lundin, Epidemiologic studies of glyphosate and cancer: A review, Regul. Toxicol. Pharmacol. 63 (2012) 440–452. doi:10.1016/j.yrtph.2012.05.012.

[21] S. Richard, S. Moslemi, H. Sipahutar, N. Benachour, G.E. Seralini, Differential effects of glyphosate and roundup on human placental cells and aromatase, Environ. Health Perspect. 113 (2005) 716–720. doi:10.1289/ehp.7728.

[22] M. Krüger, A.A. Shehata, W. Schrödl, A. Rodloff, Glyphosate suppresses the antagonistic effect of Enterococcus spp. on Clostridium botulinum, Anaerobe. 20 (2013) 74–78. doi:10.1016/j.anaerobe.2013.01.005.

[23] M. Antoniou, M.E.M. Habib, C. V Howard, R.C. Jennings, C. Leifert, R.O. Nodari, C.J. Robinson, J. Fagan, Teratogenic Effects of Glyphosate-Based Herbicides : Divergence of Regulatory Decisions from Scientific Evidence, Environ. Anal. Toxicol. (2012). doi:10.4172/2161-0525.S4-006.

[24] R. Mesnage, N. Defarge, J. Spiroux de Vendômois, G.E. Séralini, Potential toxic effects of glyphosate and its commercial formulations below regulatory limits, Food Chem. Toxicol. 84 (2015) 133–153. doi:10.1016/j.fct.2015.08.012.

[25] C. Bolognesi, S. Bonatti, P. Degan, E. Gallerani, M. Peluso, R. Rabboni, P. Roggieri, a Abbondandolo, Genotoxic activity of glyphosate and its technical formulation roundup, J. Agric. Food Chem. 45 (1997) 1957–1962. doi:Doi 10.1021/Jf9606518.

[26] C.M. Monroy, A.C. Cortés, D.M. Sicard, H.G. de Restrepo, [Cytotoxicity and genotoxicity of human cells exposed in vitro to glyphosate]., Biomédica Rev. Del Inst. Nac. Salud. 25 (2005) 335–45. http://www.ncbi.nlm.nih.gov/pubmed/16276681.

[27] S. Prasad, S. Srivastava, M. Singh, Y. Shukla, Clastogenic Effects of Glyphosate in Bone Marrow Cells of Swiss Albino Mice, J. Toxicol. 2009 (2009) 1–6. doi:10.1155/2009/308985.

[28] R. Mesnage, N. Defarge, J. Spiroux De Vendômois, G.E. Séralini, Major pesticides are more toxic to human cells than their declared active principles, Biomed Res. Int. 2014 (2014). doi:10.1155/2014/179691.

[29] US Environmental Protection Agency, Glyphosate Issue Paper: Evaluation of

Carcinogenic Potential EPA's Office of Pesticide Programs, EPA's Off. Pestic. Programs. (2016) 227.

[30] International Agency for Research on Cancer, IARC Monographs on the evaluation of carcinogenic risks to humans - volume 112: Some organophosphate insecticides and herbicides - Glyphosate, 2017. http://monographs.iarc.fr/ENG/Monographs/vol112/mono112.pdf.

[31] C. Gasnier, C. Dumont, N. Benachour, E. Clair, M. Chagnon, G. Séralini, Glyphosate-based herbicides are toxic and endocrine disruptors in human cell lines, Toxicology. 262 (2009) 184–191. doi:10.1016/j.tox.2009.06.006.

[32] N. Defarge, E. Takács, V.L. Lozano, R. Mesnage, J.S. de Vendômois, G.E. Séralini, A. Székács, Co-formulants in glyphosate-based herbicides disrupt aromatase activity in human cells below toxic levels, Int. J. Environ. Res. Public Health. 13 (2016). doi:10.3390/ijerph13030264.

[33] V. Bhardwaj, A.J. Mcgoron, Biosensor Technology for Chemical and Biological Toxins: Progress and Prospects Vinay, Phot. J. Biomed. Eng. 112 (2014) 380–392.

[34] V. Perumal, U. Hashim, Advances in biosensors: Principle, architecture and applications, J. Appl. Biomed. 12 (2014) 1–15. doi:10.1016/j.jab.2013.02.001.

[35] P. Banerjee, S. Kintzios, B. Prabhakarpandian, Biotoxin detection using cell-based sensors, Toxins (Basel). 5 (2013) 2366–2383. doi:10.3390/toxins5122366.

[36] R.P. Hollis, K. Killham, Design and Application of a Biosensor for Monitoring Toxicity of Compounds to Eukaryotes, Appl. Environ. Microbiol. 66 (2000) 1676–1679.

[37] G. Zhao, H. Wang, G. Liu, Advances in Biosensor-Based Instruments for Pesticide Residues Rapid Detection, Int. J. Electrochem Sci. 10 (2015) 9790–9807.

[38] I. Székács, R. Horvath, A. Székács, Label-Free Optical Biosensors for Monitoring Cellular Processes and Cytotoxic Agents at Interfaces Using Guided Modes and Advanced Phase-Contrast Imaging Techniques, in: 2016: pp. 443–468. doi:10.1007/978-3-319-28926-7_21.

[39] C. Xiao, J.H.T. Luong, Assessment of cytotoxicity by emerging impedance spectroscopy, Toxicol. Appl. Pharmacol. 206 (2005) 102–112. doi:10.1016/j.taap.2004.10.025.

[40] H.R. Siddiquei, A.N. Nordin, M.A. Arifin, N.H. Sulong, I. Voiculescu, Electrical Cell-substrate Impedance Sensing (ECIS) based Biosensor for Characterization of DF-1 Cells, ICCCE. 6 (2010) 11–13.

[41] E. Primiceri, M.S. Chiriacò, E. D'Amone, E. Urso, R.E. Ionescu, A. Rizzello, M. Maffia, R. Cingolani, R. Rinaldi, G. Maruccio, Real-time monitoring of copper ions-induced cytotoxicity by EIS cell chips, Biosens. Bioelectron. 25 (2010) 2711–2716. doi:10.1016/j.bios.2010.04.032.

[42] S. ALPAT, S. ALPAT, B. CADIRCI, I. YASA, A. TELEFONCU, A novel microbial biosensor based on Circinella sp. modified carbon paste electrode and its voltammetric application, Sensors Actuators B Chem. 134 (2008) 175–181. doi:10.1016/j.snb.2008.04.044.

[43] X. Zhu, G. Wu, N. Lu, X. Yuan, B. Li, A miniaturized electrochemical toxicity biosensor based on graphene oxide quantum dots/carboxylated carbon nanotubes for assessment of priority pollutants, J. Hazard. Mater. 324 (2017) 272–280. doi:10.1016/j.jhazmat.2016.10.057.

[44] Y. Lei, P. Mulchandani, J. Wang, W. Chen, A. Mulchandani, Highly Sensitive and Selective Amperometric Microbial Biosensor for Direct Determination of p-Nitrophenyl-Substituted Organophosphate Nerve Agents, Environ. Sci. Technol. 39 (2005) 8853–8857. http://pubs.acs.org/doi/abs/10.1021/es050720b.

[45] X. Wang, M. Liu, X. Wang, Z. Wu, L. Yang, S. Xia, L. Chen, J. Zhao, P-benzoquinone-mediated amperometric biosensor developed with Psychrobacter sp. for toxicity testing of heavy metals, Biosens. Bioelectron. 41 (2013) 557–562. doi:10.1016/j.bios.2012.09.020.

[46] G. Hughes, R.M. Pemberton, P.R. Fielden, J.P. Hart, A novel reagentless glutamate microband biosensor for real-time cell toxicity monitoring, Anal. Chim. Acta. 933 (2016) 82–88. doi:10.1016/j.aca.2016.06.005.

[47] Y. Wang, Q. Chen, X. Zeng, Potentiometric biosensor for studying hydroquinone cytotoxicity in vitro, Biosens. Bioelectron. 25 (2010) 1356–1362. doi:10.1016/j.bios.2009.10.027.

[48] K.M.L. May, Y. Wang, L.G. Bachas, K.W. Anderson, Development of a whole-cell-based biosensor for detecting histamine as a model toxin, Anal. Chem. 76 (2004) 4156–4161. doi:10.1021/ac049810+.

[49] D. Grieshaber, R. MacKenzie, J. Vörös, E. Reimhult, Electrochemical Biosensors - Sensor Principles and Architectures, Sensors. 8 (2008) 1400–1458. doi:10.3390/s8031400.

[50] K.A. Marx, T. Zhou, A. Montrone, H. Schulze, S.J. Braunhut, A quartz crystal microbalance cell biosensor: Detection of microtubule alterations in living cells at nM nocodazole concentrations, in: Biosens. Bioelectron., 2001: pp. 773–782. doi:10.1016/S0956-5663(01)00219-6.

[51] S. Zhang, H. Bai, J. Pi, P. Yang, J. Cai, Label-free quartz crystal microbalance with dissipation monitoring of resveratrol effect on mechanical changes and folate receptor expression levels of living MCF-7 cells: A model for screening of drugs, Anal. Chem. 87 (2015) 4797–4805. doi:10.1021/acs.analchem.5b00083.

[52] M.M. Chisti, L. Tan, J.F. Klamerus, P. Lin, I. Jaiyesimi, A. Rehman, X. Zeng, Quartz crystal microbalance (QCM) piezo-immunosensors: A novel technique to study CD20 antigen interaction with rituximab and its clinical implications, Blood. 124 (2014) 1–4. http://www.embase.com/search/results?subaction=viewrecord&from=export&id=L71762388.

[53] O. Maglio, S. Costanzo, R. Cercola, G. Zambrano, M. Mauro, R. Battaglia, G. Ferrini, F. Nastri, V. Pavone, A. Lombardi, A Quartz Crystal Microbalance Immunosensor for Stem Cell Selection and Extraction, Sensors. 17 (2017) 2747. doi:10.3390/s17122747.

[54] G. Wang, A.H. Dewilde, J. Zhang, A. Pal, M. Vashist, D. Bello, K.A. Marx, S.J. Braunhut, J.M. Therrien, A living cell quartz crystal microbalance biosensor for continuous monitoring of cytotoxic responses of macrophages to single-walled carbon nanotubes, (2011) 1–17.

[55] J.Y. Chen, L.S. Penn, J. Xi, Quartz crystal microbalance: Sensing cell-substrate adhesion and beyond, Biosens. Bioelectron. 99 (2018) 593–602. doi:10.1016/j.bios.2017.08.032.

[56] I. Székács, Á. Fejes, S. Klátyik, E. Takács, D. Patkó, J. Pomóthy, M. Mörtl, R. Horváth, E. Madarász, B. Darvas, A. Székács, Environmental and Toxicological Impacts of Glyphosate with Its Formulating Adjuvant, Int. J. Biol. Vet. 8 (2014) 213–218.

[57] B. Peter, J. Nador, K. Juhasz, A. Dobos, L. Korosi, I. Székács, D. Patko, R. Horvath, Incubator proof miniaturized Holomonitor to in situ monitor cancer cells exposed to green tea polyphenol and preosteoblast cells adhering on nanostructured titanate surfaces: validity of the measured parameters and their corrections, J. Biomed. Opt. 20 (2015) 67002. doi:10.1117/1.JBO.20.6.067002.

[58] J. Kühn, E. Shaffer, J. Mena, B. Breton, J. Parent, B. Rappaz, M. Chambon, Y. Emery, P. Magistretti, C. Depeursinge, P. Marquet, G. Turcatti, Label-Free Cytotoxicity Screening Assay by Digital Holographic Microscopy, Assay Drug Dev. Technol. 11 (2013) 101–107. doi:10.1089/adt.2012.476.

[59] A. Mölder, M. Sebesta, M. Gustafsson, L. Gisselson, A.G. Wingren, K. Alm, Non-invasive, label-free cell counting and quantitative analysis of adherent cells using digital holography, J. Microsc. 232 (2008) 240–247. doi:10.1111/j.1365-2818.2008.02095.x.

[60] J.W. Choi, K.W. Park, D.B. Lee, W. Lee, W.H. Lee, Cell immobilization using self-assembled synthetic oligopeptide and its application to biological toxicity detection using surface plasmon resonance, in: Biosens. Bioelectron., 2005: pp. 2300–2305. doi:10.1016/j.bios.2004.11.019.

[61] V. Chabot, C.M. Cuerrier, E. Escher, V. Aimez, M. Grandbois, P.G. Charette, Biosensing based on surface plasmon resonance and living cells, Biosens. Bioelectron. 24 (2009) 1667–1673. doi:10.1016/j.bios.2008.08.025.

[62] H. Andersson, B. Kågedal, C.-F. Mandenius, Monitoring of troponin release from cardiomyocytes during exposure to toxic substances using surface plasmon resonance biosensing., Anal. Bioanal. Chem. 398 (2010) 1395–402. doi:10.1007/s00216-010-4041-9.

[63] V. Chabot, Y. Miron, M. Grandbois, P.G. Charette, Long range surface plasmon resonance for increased sensitivity in living cell biosensing through greater probing depth, Sensors Actuators, B Chem. 174 (2012) 94–101. doi:10.1016/j.snb.2012.08.028.

[64] Y. Wang, S. Zhang, C. Zhang, Z. Zhao, X. Zheng, L. Xue, J. Liu, X. Yuan, Investigation of an SPR biosensor for determining the influence of connexin 43 expression on the cytotoxicity of cisplatin †, (2016) 3411–3420. doi:10.1039/c6an00264a.

[65] J. Vörös, R. Graf, G.L. Kenausis, A. Bruinink, J. Mayer, M. Textor, E. Wintermantel, N.D. Spencer, Feasibility study of an online toxicological sensor based on the optical waveguide technique., Biosens. Bioelectron. 15 (2000) 423–9. http://www.ncbi.nlm.nih.gov/pubmed/11419636.

[66] T.S. Hug, J.E. Prenosil, M. Morbidelli, Optical waveguide lightmode spectroscopy as a new method to study adhesion of anchorage-dependent cells as an indicator of

metabolic state, Biosens. Bioelectron. 16 (2001) 865–874. doi:10.1016/S0956-5663(01)00204-4.

[67] T.S. Hug, J.E. Prenosil, P. Maier, M. Morbidelli, On-line monitoring of adhesion and proliferation of cultured hepatoma cells using optical waveguide lightmode spectroscopy (OWLS)., Biotechnol. Prog. 18 (2002) 1408–13. doi:10.1021/bp025554f.

[68] L.L. Chan, S.L. Gosangari, K.L. Watkin, B.T. Cunningham, High throughput cytotoxicity screening using photonic crystal biosensors, in: TRANSDUCERS EUROSENSORS '07 - 4th Int. Conf. Solid-State Sensors, Actuators Microsystems, IEEE, 2007: pp. 799–802. doi:10.1109/SENSOR.2007.4300251.

[69] S.M. Shamah, B.T. Cunningham, Label-free cell-based assays using photonic crystal optical biosensors, Analyst. 136 (2011) 1090. doi:10.1039/c0an00899k.

[70] L.L. Chan, S.L. Gosangari, K.L. Watkin, B.T. Cunningham, A label-free photonic crystal biosensor imaging method for detection of cancer cell cytotoxicity and proliferation, Apoptosis. 12 (2007) 1061–1068. doi:10.1007/s10495-006-0031-y.

[71] S. George, S. V. Bhalerao, E.A. Lidstone, I.S. Ahmad, A. Abbasi, B.T. Cunningham, K.L. Watkin, Cytotoxicity screening of Bangladeshi medicinal plant extracts on pancreatic cancer cells, BMC Complement. Altern. Med. 10 (2010) 1–11. doi:10.1186/1472-6882-10-52.

[72] Y. Fang, A.M. Ferrie, N.H. Fontaine, J. Mauro, J. Balakrishnan, Resonant Waveguide Grating Biosensor for Living Cell Sensing, Biophys. J. 91 (2006) 1925–1940. doi:10.1529/biophysj.105.077818.

[73] G. Li, F. Lai, Y. Fang, Modulating Cell-Cell Communication with a High-Throughput Label-Free Cell Assay, (2012). doi:10.1177/2211068211424548.

[74] Y. Nazirizadeh, V. Behrends, N. Orgovan, R. Horvath, Intensity interrogation near cutoff resonance for label-free cellular profiling, Sci. Rep. (2016) 1–6. doi:10.1038/srep24685.

[75] H.-P. Song, H. Wang, X. Zhao, L. He, H. Zhong, S.-Q. Wu, P. Li, H. Yang, Label-free pharmacological profiling based on dynamic mass redistribution for characterization and authentication of hazardous natural products, J. Hazard. Mater. 333 (2017) 265–274. doi:10.1016/j.jhazmat.2017.03.025.

[76] R. Horvath, H.C. Pedersen, N. Skivesen, C. Svanberg, N.B. Larsen, Fabrication of reverse symmetry polymer waveguide sensor chips on nanoporous substrates using dip-floating, J. Micromechanics Microengineering. 15 (2005) 1260–1264. doi:10.1088/0960-1317/15/6/017.

[77] R. Horvath, K. Cottier, H.C. Pedersen, J.J. Ramsden, Multidepth screening of living cells using optical waveguides, Biosens. Bioelectron. 24 (2008) 799–804. doi:10.1016/j.bios.2008.06.059.

[78] N. Orgovan, B. Peter, S. Bosze, J.J. Ramsden, B. Szabo, R. Horvath, Dependence of cancer cell adhesion kinetics on integrin ligand surface density measured by a high-throughput label-free resonant waveguide grating biosensor, Sci. Rep. 4 (2014) 4034. doi:10.1038/srep04034.

[79] N. Orgovan, R. Ungai-Salánki, S. Lukácsi, N. Sándor, Z. Bajtay, A. Erdei, B. Szabó, R. Horvath, Adhesion kinetics of human primary monocytes, dendritic cells, and

macrophages: Dynamic cell adhesion measurements with a label-free optical biosensor and their comparison with end-point assays, Biointerphases. 11 (2016) 31001. doi:10.1116/1.4954789.

[80] I. Kurucz, B. Peter, A. Prosz, I. Szekacs, R. Horvath, A. Erdei, Label-free optical biosensor for on-line monitoring the integrated response of human B cells upon the engagement of stimulatory and inhibitory immune receptors, Sensors Actuators, B Chem. 240 (2017) 528–535. doi:10.1016/j.snb.2016.09.015.

[81] B. Peter, E. Farkas, E. Forgacs, A. Saftics, B. Kovacs, S. Kurunczi, I. Szekacs, A. Csampai, S. Bosze, R. Horvath, Green tea polyphenol tailors cell adhesivity of RGD displaying surfaces: multicomponent models monitored optically, Sci. Rep. 7 (2017) 42220. doi:10.1038/srep42220.

[82] Y. Fang, Label-Free Cell-Based Assays with Optical Biosensors in Drug Discovery, (2017). doi:10.1089/adt.2006.4.583.

[83] G.M. Williams, R. Kroes, I.C. Munro, Safety Evaluation and Risk Assessment of the Herbicide Roundup 1 and Its Active Ingredient, Glyphosate, for Humans, World Health. 165 (2000) 117–165. doi:10.1006/rtph.1999.1371.

[84] S.M. Bradberry, A.T. Proudfoot, J.A. Vale, Glyphosate poisoning, Toxicol. Rev. 23 (2004) 159–167. doi:10.2165/00139709-200423030-00003.

[85] S. Kustermann, F. Boess, A. Buness, M. Schmitz, M. Watzele, T. Weiser, T. Singer, L. Suter, A. Roth, A label-free, impedance-based real time assay to identify drug-induced toxicities and differentiate cytostatic from cytotoxic effects, Toxicol. Vitr. 27 (2013) 1589–1595. doi:10.1016/j.tiv.2012.08.019.

[86] N. Orgovan, B. Kovacs, E. Farkas, B. Szabó, N. Zaytseva, Y. Fang, R. Horvath, Bulk and surface sensitivity of a resonant waveguide grating imager, Appl. Phys. Lett. 104 (2014) 0–4. doi:10.1063/1.4866460.

[87] H. Seibert, S. Mörchel, M. Gülden, Factors influencing nominal effective concentrations of chemical compounds in vitro: medium protein concentration, Toxicol. Vitr. 16 (2002) 289–297. doi:10.1016/S0887-2333(02)00014-0.

[88] M. Bollinger, F. Manzenrieder, R. Kolb, A. Bochen, S. Neubauer, L. Marinelli, V. Limongelli, E. Novellino, G. Moessmer, R. Pell, W. Lindner, J. Fanous, A. Hoffman, H. Kessler, Tailoring of integrin ligands: Probing the charge capability of the metal ion-dependent adhesion site, J. Med. Chem. 55 (2012) 871–882. doi:10.1021/jm2013826.

[89] D. Hedberg, M. Wallin, Toxicology in Vitro Effects of Roundup and glyphosate formulations on intracellular transport , microtubules and actin filaments in Xenopus laevis melanophores, Toxicol. Vitr. 24 (2010) 795–802. doi:10.1016/j.tiv.2009.12.020.

[90] C.W.G. and K.R. Ayscough, Abstract, The actin cytoskeleton : a key regulator of apoptosis and ageing ?, Mol. Cell Biol. 6 (2005) 583–589.

[91] A.D.F. Toy, E.H. Uhing, Aminomethylenephosphonic acids, salts thereof, and process for their production, 1964. http://1.usa.gov/1BULtJj.

[92] S.O. Duke, J. Lydon, W.C. Koskinen, T.B. Moorman, R.L. Chaney, R. Hammerschmidt, Glyphosate Effects on Plant Mineral Nutrition, Crop Rhizosphere Microbiota, and Plant Disease in Glyphosate-Resistant Crops, (2012).

doi:10.1021/jf302436u.

[93] N. Benachour, G. Se, Glyphosate Formulations Induce Apoptosis and Necrosis in Human Umbilical , Embryonic , and Placental Cells, Chem. Res. Toxicol. 22 (2009) 97–105. doi:10.1021/tx800218n.

[94] HoloMonitor application note on label-free toxicology, (n.d.). http://www.phiab.se/reports/2014/ToxicologyAppNotePHI-140919.pdf (accessed July 21, 2017).

[95] R. Mesnage, B. Bernay, G.E. Séralini, Ethoxylated adjuvants of glyphosate-based herbicides are active principles of human cell toxicity, Toxicology. 314 (2013) 122–128. doi:10.1016/j.tox.2012.09.006.

Figure captions

Figure 1. MC3T3-E1 cell response to the treatment with xenobiotics. Typical biosensor responses obtained from a representative experiment after MC3T3-E1 cells were exposed to 0.1% Roundup Classic, 0.016% POEA, and 0.042% glyphosate (equivalents of 0.1% Roundup solution) in α-MEM+10% FBS **(A)** or in 20 mM HEPES HBSS buffer **(B)**. Each data point represents the mean and the standard deviation of the average value of data obtained in triplicates. Dose response curves on MC3T3-E1 cells in α-MEM+10% FBS **(C)** or in 20 mM HEPES HBSS buffer (**D**). Data represented are mean ± SD of identical experiments made in three replicates.

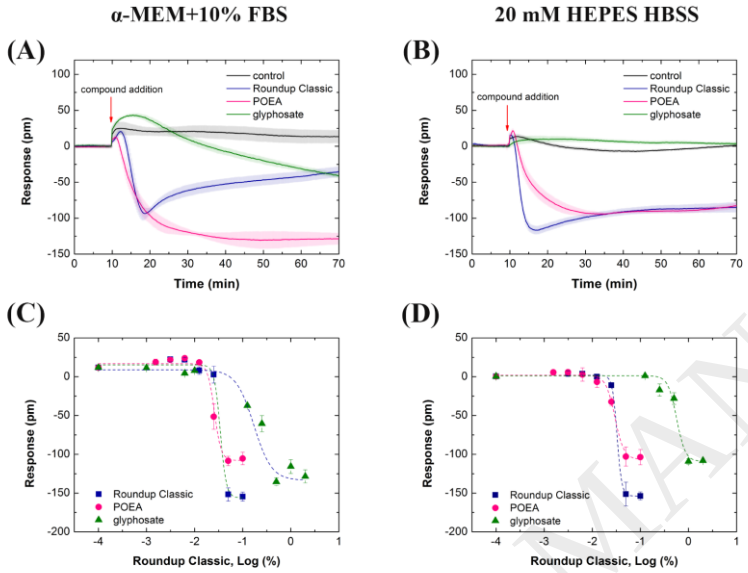

Figure 2. Fluorescent images of cell cytoskeleton and focal adhesions. (**A)** untreated cells (control), **(B)** 0.42% glyphosate, **(C)** 0.02% POEA, and **(D)** 0.1% Roundup Classic. Blue color: cell nuclei; red color: F-actin; green color: vinculin. Scale bars: 50 μm.

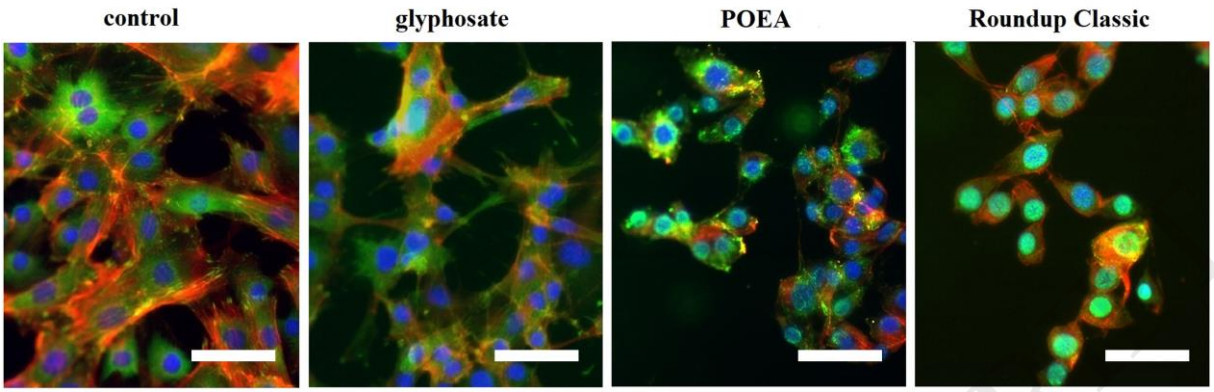

Figure 3. Time-dependent morphological changes in MC3T3-E1 cells, detected by phase contrast holographic microscopy. (**A**) untreated cells, (**B**) 0.02% Roundup Classic, (**C**) 0.003% POEA, (**D**) 0.008% glyphosate and (**E**) 0.5% glyphosate.

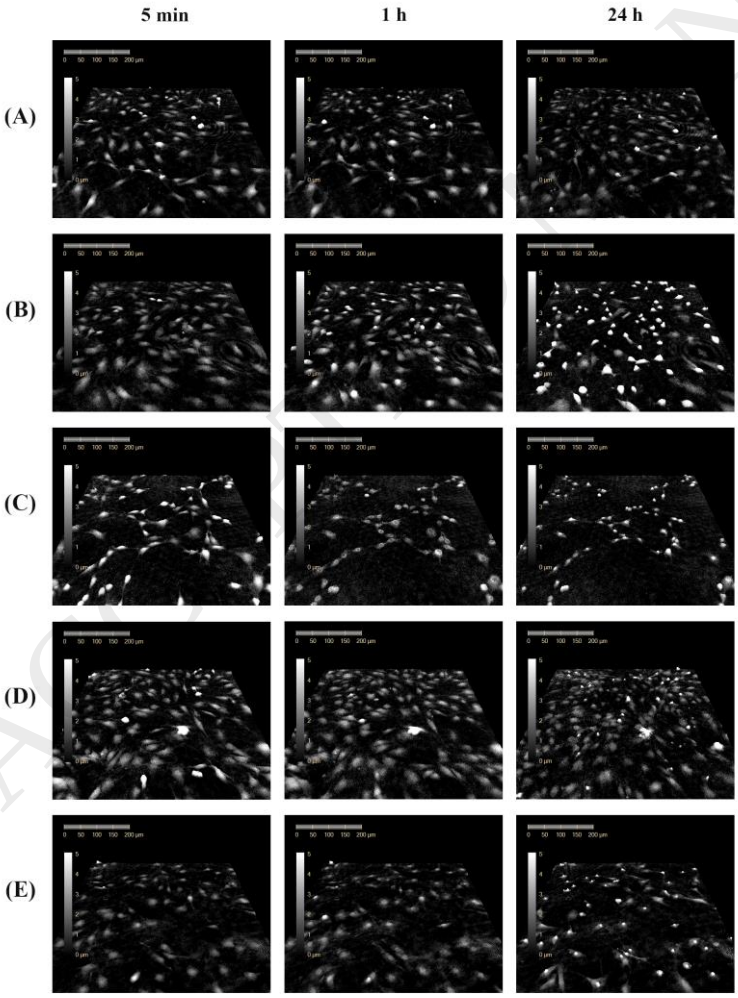

Figure 4. The analysis of holographic microscopy data: (**A**) MC3T3-E1 cells proliferation, (**B**) migration dynamic and (**C**) cell optical thickness changes under exposure of xenobiotics.

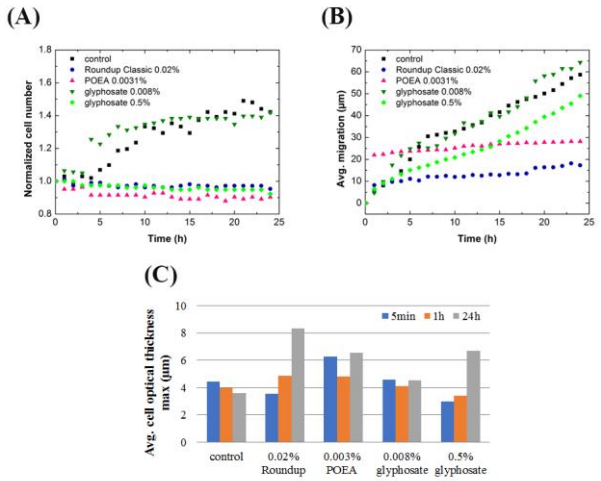

Figure 5. Apoptosis induced in MC3T3-E1 cells by xenobiotics. (**A**) Muse measurement setup, (**B**) caspase 3/7 apoptosis profile (data shown correspond to concentrations near the IC_{50} values for Roundup Classic and POEA, and to the highest applied concentrations for glyphosate), and (**C**) dose response curves.

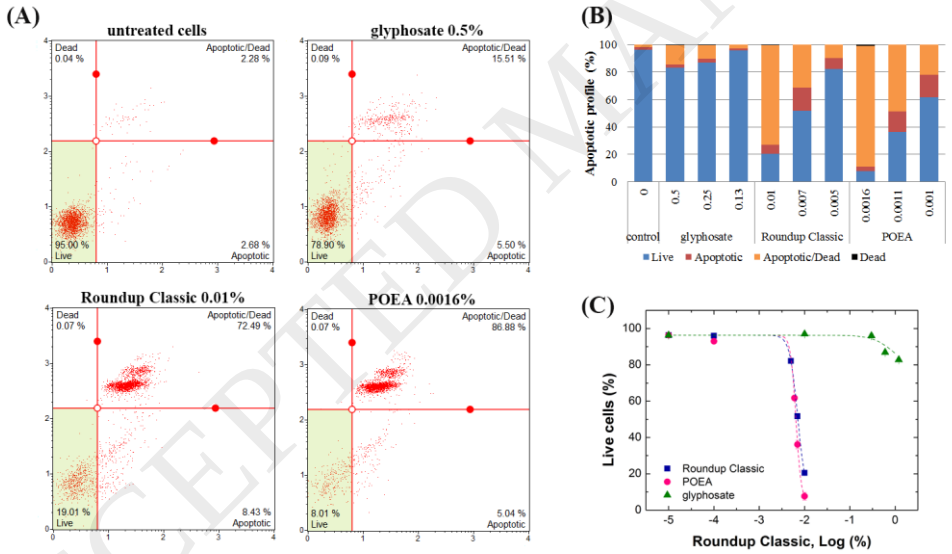

Table 1. IC_{50} values upon 1 h of exposure. Data represent mean ± SD of two identical experiments made in three replicates.

Component	in α-MEM+10% FBS			in 20 mM HEPES HBSS		
	actual concentration		equivalent to diluted Roundup Classic solution (%)	actual concentration		equivalent of diluted Roundup Classic solution (%)
	(%)	(mM)		(%)	(mM)	
Roundup Classic	0.024±0.011	0.04±0.02 (POEA) 0.44±0.20 (glyphosate)	**0.024**±0.011	0.028±0.012	0.05±0.02 (POEA) 0.51±0.22 (glyphosate)	**0.028**±0.012
POEA	0.003±0.001	0.03±0.01	**0.021**±0.004	0.003±0.002	0.03±0.02	**0.019**±0.010
glyphosate	0.068±0.004	2.98±0.18	**0.163**±0.010	0.223±0.022	9.77±0.96	**0.538**±0.052